Journal of Cerebral Blood Flow & Metabolism (2011) 31, 2293–2301

www.jcbfm.com

GSM mobile phone radiation suppresses brain glucose metabolism

Myoung Soo Kwon[1], Victor Vorobyev[1], Sami Kännälä[2], Matti Laine[3], Juha O Rinne[4], Tommi Toivonen[2], Jarkko Johansson[4], Mika Teräs[4], Harri Lindholm[5], Tommi Alanko[5] and Heikki Hämäläinen[1]

[1]*Department of Psychology, Centre for Cognitive Neuroscience, University of Turku, Turku, Finland;* [2]*STUK—Radiation and Nuclear Safety Authority, Helsinki, Finland;* [3]*Department of Psychology and Logopedics, Åbo Akademi University, Turku, Finland;* [4]*Turku PET Centre, Turku University Hospital, Turku, Finland;* [5]*Finnish Institute of Occupational Health, Helsinki, Finland*

We investigated the effects of mobile phone radiation on cerebral glucose metabolism using high-resolution positron emission tomography (PET) with the ^{18}F-deoxyglucose (FDG) tracer. A long half-life (109 minutes) of the ^{18}F isotope allowed a long, natural exposure condition outside the PET scanner. Thirteen young right-handed male subjects were exposed to a pulse-modulated 902.4 MHz Global System for Mobile Communications signal for 33 minutes, while performing a simple visual vigilance task. Temperature was also measured in the head region (forehead, eyes, cheeks, ear canals) during exposure. ^{18}F-deoxyglucose PET images acquired after the exposure showed that relative cerebral metabolic rate of glucose was significantly reduced in the temporoparietal junction and anterior temporal lobe of the right hemisphere ipsilateral to the exposure. Temperature rise was also observed on the exposed side of the head, but the magnitude was very small. The exposure did not affect task performance (reaction time, error rate). Our results show that short-term mobile phone exposure can locally suppress brain energy metabolism in humans.
Journal of Cerebral Blood Flow & Metabolism (2011) **31,** 2293–2301; doi:10.1038/jcbfm.2011.128; published online 14 September 2011

Keywords: cellular phone; electromagnetic field; fluorodeoxyglucose; positron emission tomography; radio frequency

Introduction

The use of mobile phones continues to expand worldwide but possible effects of mobile phone radiation on brain function remain unclear. A large number of behavioral and electrophysiological studies have been conducted but with inconsistent results (see Kwon and Hämäläinen, 2011, for a review). Earlier behavioral studies, for example, reported faster response speed in attention or working memory tasks (Preece *et al*, 1999; Koivisto *et al*, 2000*a*, *b*; Edelstyn and Oldershaw, 2002), but later more stringent studies (e.g., with corrections for multiple comparisons) failed to replicate such findings. Results of electroencephalography studies have also been contradictory particularly in the α band: some studies reported increased α activity (Croft *et al*, 2002, 2008; Curcio *et al*, 2005; Regel *et al*, 2007), while others found no such effects (Röschke and Mann, 1997; Hietanen *et al*, 2000; Perentos *et al*, 2007; Kleinlogel *et al*, 2008). Among brain imaging methods, positron emission tomography (PET) is particularly suitable because it allows metal parts inside the scanner. Nevertheless, PET has rarely been used in this field (Huber *et al*, 2002, 2005; Haarala *et al*, 2003; Aalto *et al*, 2006; Mizuno *et al*, 2009) and these few studies, mainly on cerebral blood flow (CBF) measured with the ^{15}O-water tracer, produced contradictory results.

In previous [^{15}O]H_2O-PET studies, Huber *et al* (2002, 2005) found increased CBF in the prefrontal cortex after a 30-minute exposure to a 900-MHz Global System for Mobile Communications (GSM) signal. However, the specific areas of activation were inconsistent between the two studies, and the locations of CBF change did not correspond to the distribution of maximal radiation energy absorption. In addition, a 10-minute interval between phone exposure and subsequent scanning makes the relationship between exposure and CBF responses questionable. In contrast, Aalto *et al* (2006) acquired [^{15}O]H_2O-PET scans during a continuous 51 minutes

Correspondence: Dr MS Kwon, Department of Psychology, Centre for Cognitive Neuroscience, University of Turku, Assistentinkatu 7, 20014 Turku, Finland.
E-mail: mskwon@utu.fi
This study was funded by Finnish National Technology Agency (Tekes).
Received 9 May 2011; revised 19 July 2011; accepted 26 July 2011; published online 14 September 2011

exposure to a 902-MHz GSM signal and found decreased CBF in the temporal cortex near the exposure source.

Here, we measured relative cerebral metabolic rate of glucose (CMRglu) to trace brain activation (Chang *et al*, 1987). Cerebral metabolic rate of glucose and CBF are closely coupled (Fox *et al*, 1988) but represent different physiological processes: CMRglu is a more direct marker of neural activity than CBF. Brain activation studies based on glucose consumption are rather rare but have proved advantageous in certain cases (Harris *et al*, 2005). The FDG labeled with the ^{18}F isotope of a 109-minute long half-life (cf. ^{15}O isotope of 2 minutes half-life) is mostly (70% to 80%) taken up by brain tissue in 30 to 40 minutes after tracer injection (Phelps *et al*, 1979) and the concentration of the phosphorylated FDG trapped inside brain cells remains relatively constant for about 2 hours. Therefore, exposure and scan periods can be separated (Figure 1), approximately coinciding with the FDG accumulation and steady-state FDG concentration phases, respectively. This allowed 30 minutes long exposure outside the PET scanner, thus making exposure conditions more natural than when measuring CBF. The relatively long half-life of the ^{18}F also allowed sufficient time to gather considerable count rates, so as to produce high-quality images of the FDG distribution.

There is only one previous FDG-PET study on cell phone field effects (Volkow *et al*, 2011). It reported an increase in CMRglu in the brain regions closest to the active handset. However, the methodology of the study and the reporting of the results have evoked considerable criticism (Kosowsky *et al*, 2011; Davis and Balzano, 2011; Nordström, 2011) and therefore further FDG-PET studies are called for.

In the present study, 13 young healthy right-handed male subjects were real- and sham-exposed (ON and OFF conditions, respectively) to a 902.4-MHz GSM signal to the right side of the head for 30 minutes, while performing a simple visual vigilance task to minimize differences in cognitive states between exposure conditions. Temperature was also measured in the head region during exposure for possible temperature rise due to phone radiation (Figure 2). After 30 minutes exposure when the injected FDG was mostly taken up by the brain tissue, a 30-minute whole-brain emission scan was acquired to depict the brain state during the exposure.

Materials and methods

Subjects and Out-Of-Scanner Procedure

The study protocol was approved by the ethics committee of the Hospital District of Southwest Finland, and the study was performed according to the Declaration of Helsinki. Subjects were 13 right-handed male volunteers aged 21 to 29 years (mean ± s.d. = 24.5 ± 2.8) without history of neurologic or psychiatric problems, or permanent medications. They gave an informed consent and were paid 200 euros for their participation.

Subjects participated in two sessions of real and sham exposure conditions at and interval of at least 6 days (mean ± s.d. = 13.6 ± 8.6). The two conditions were counterbalanced across subjects in a double-blind manner. Subjects fasted for at least 8 hours before the experiment to stabilize blood glucose concentration. An intravenous catheter was inserted into the left antecubital vein for tracer injection and blood sampling. Subject sat in a comfortable chair with armrests in a dim-lighted quiet room. A 33-minute exposure started 3 minutes after intravenous bolus injection of ~200 MBq FDG.

Behavioral Task

Subjects performed a simple visual match-to-sample (0-back) vigilance task during exposure to minimize

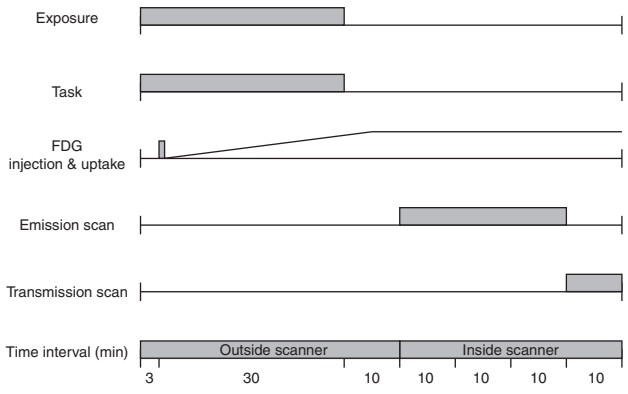

Figure 1 Timeline of the ^{18}F-deoxyglucose (^{18}F-FDG) experiment. The figure shows one emission scan following either real or sham exposure. The second scan was performed on a different day with the same protocol but with the other exposure condition.

Figure 2 Frontal view of a subject and the exposure setup. Two modified phones attached to a plastic helmet were placed against each ear, mimicking the natural position during mobile phone use. Five temperature probes were attached to the head skin with adhesive tape, and three of them are shown here on the forehead and at both outer eye corners.

differences in cognitive states between exposure conditions. A laptop computer was set on the table and the computer screen was 1 m away from the face of the subject. Stimuli were circles (2 cm in diameter) of four different colors (red, green, blue, and yellow) presented in a random order in the center of the computer screen for 0.5 seconds at random 2 to 5 seconds onset-to-onset intervals with a central fixation cross. Subjects responded only to the target color (red, $P = 0.25$) by pressing a mouse button with the right index finger as soon as possible. Stimulus presentation and response registration was controlled by Presentation software (Neurobehavioral Systems, Albany, CA, USA).

Exposure Setup

Two modified phones attached to a plastic helmet were placed against the ears (Figure 2), but only the phone on the right side transmitted the signal in the real exposure (ON) condition, while an identical dummy phone on the left side was inactive. The model of the phone used for the exposure was Nokia 6110 (Espoo, Finland). The exposing phone was modified to eliminate temperature rise of the phone chassis and to maintain a constant output power. The transmitter of the exposing phone was deactivated, battery and loudspeaker were removed, and antenna input was replaced by an external coaxial cable. The signal was taken from an identical phone, which was controlled by a service software (WinTesla v. 6.03, Nokia) to continuously transmit a typical GSM voice-call signal. The signal consisted of 0.577 milliseconds bursts of 902.4 MHz carrier frequency (GSM channel # 62) repeated every 4.615 milliseconds. The power level was adjusted with an amplifier (R720F, RF Power Labs, Woodinville, WA, USA) and the signal was fed to the antenna of the exposing phone with a coaxial cable. Transmitted and reflected power levels were monitored during exposures with an RF power meter (NAS Z7, Rohde and Schwartz, Munich, Germany). The power control instrumentation was connected to the exposing phone via a 6-m long cable and placed in a separate room. Therefore, any acoustic stimulus caused by the instrumentation was eliminated.

To assess the correct input power, specific absorption rate (SAR) values for the exposing phones were measured as specified in IEC 62209-1 (IEC, 2005). The phones were placed against the ear of a standard anthropomorphic mannequin (SAM) and SAR was measured with a dosimetric scanning system (DASY4, Schmid and Partner Engineering AG, Zurich, Switzerland). The SAM phantom was filled with head tissue simulating liquid ($\sigma = 1.023$ S/m, $\varepsilon_r = 42.01$, $\rho = 1{,}000$ kg/m^3). The aimed 10 g averaged SAR level (SAR_{10g}) was 1 W/kg. The corresponding input power was 240 mW, which was similar to the maximum output power of standard GSM phones. The final measured SAR_{10g} values were 1.1 W/kg (left) and 1.0 W/kg (right), and 1 g averaged SAR (SAR_{1g}) values were 1.5 W/kg (left) and 1.4 W/kg (right).

Before exposures, the return loss for the exposing phone was measured with a network analyzer (HP 8752C, Hewlett-Packard, Santa Clara, CA, USA) to ensure that the external antenna feeding was properly attached. The measurements were performed at both sides of the SAM phantom and the average return loss was 21 dB at 902.4 MHz. Hence, the feeding was operating as intended and the antenna matching was adequate.

Specific Absorption Rate Evaluation

Microwave exposure of tissue is expressed in terms of SAR, which describes the dissipated power in a mass unit. Numerical simulations were performed to evaluate the SAR distribution. Possible effects of metallic parts of the temperature probes on the SAR distribution were also examined. Simulations were performed at the same frequency of 902.4 MHz used in the exposure with commercial finite-difference time-domain software (SEMCAD X v. 14.2, Schmid and Partner Engineering AG). The results were visualized with open-source software (ParaView v. 3.8, Kitware, Clifton Park, NY, USA).

The numerical model of the exposure setup consisted of 94×10^6 nonuniformly sized and spaced voxels. The human model used in the calculations was a magnetic resonance imaging (MRI)-based model Duke (a 34-year-old European male) of the Virtual Family (Christ *et al*, 2010) that was cut at the shoulder level. The basic voxel size of the head model was $1 \times 1 \times 1$ mm^3. Dielectric parameters for the 45 tissues in the head model were taken from the data in Gabriel (1996).

The source model was based on the computer-aided design data of the exposing phone provided by the manufacturer. The phones were placed in the same locations as in exposures. The calculation grid was reduced to 0.2 mm for the antenna element of the exposing phone. The dummy phone was modeled with a coarser grid. Dielectric properties of the phones were the same as in Boutry *et al* (2008).

The temperature probes were modeled as 2 mm thick metallic wires. The probes inside the ear canals were coated with an insulator. All the metallic parts in the numerical model were treated as perfect electric conductors.

The numerical phone model was validated by simulating the exposure on a numerical SAM model. The phone model was placed against the right ear of the SAM model and the SAR distribution was evaluated. The simulated SAR_{1g} and SAR_{10g} values differed from the measured values by $< 7.6\%$ and 4.9%, respectively. Moreover, the simulated return losses and center frequencies agreed well. The quality of the source model was therefore considered as adequate.

The uncertainty of the dosimetry was assessed by running multiple simulations with the model modified according to actual positioning accuracies and anatomical variations among individuals. The uncertainty of the instrumentation was also analyzed. The main factors contributing to the uncertainty of the dosimetry are postural changes during exposure, differences in head anatomy, uncertainty in incident power, and numerical uncertainties (Kuster *et al*, 2004). The uncertainty due to phone positioning was assessed to be $\pm 9\%$. The variation in SAR due to different head sizes was assessed by scaling

the head model ±10%. Based on the simulations, differences in head anatomy produced an uncertainty of ±9%. The uncertainty in incident power was assessed to be ±10%. The numerical uncertainties result from, for example, uncertainty in dielectric properties and staircasing errors. The order of magnitude of these errors was estimated to be ±10%. The expanded uncertainty for the dosimetry was ±20% at 95% confidence interval.

Temperature Measurements

Temperature was measured in the head region at 1-minute intervals during exposure for possible temperature rise due to phone radiation. Five surface temperature probes (YSI 409A, Measurement Specialties, Hampton, VA, USA) were placed on the face of the subject (Figure 2): one on the forehead, two at the outer eye corners, and two on the cheeks in the middle between the outer eye corner and the mouth corner. Two probes (YSI 555, Measurement Specialties) were inserted into the ear canals. Temperature data were recorded by the loggers (Veriteq Instruments, Type 1400, Richmond, Canada) placed on the subject's waist.

Anatomical Imaging

Before the experiment, a high-resolution T1-weighted anatomical image was acquired from each subject using a Philips Gyroscan Intera 1.5 T CV Novo Dual MRI Scanner (Philips Healthcare, Best, The Netherlands) with a standard head coil (repetition time = 25 milliseconds, echo time = 4.6 milliseconds, flip angle = 30°, voxel size = $1.09 \times 1.09 \times 0.5\,mm^3$, matrix size = 256×256, field of view = $27.9\,cm^2$). The MRI images were used to check for brain abnormalities and served as anatomical references in PET data processing.

Positron Emission Tomography Data

Acquisition: After the exposure, the phones and temperature probes were removed and the subject was placed into the high-resolution PET scanner (ECAT HRRT, Siemens CTI, Knoxville, TN, USA) (Wienhard *et al*, 2002). The head of the subject was fixed to the headrest of the scanner with an individual thermoplastic mask made before the experiment. An external position tracker (Polaris Vicra, Northern Digital Inc., Waterloo, Canada) monitored the head movement during emission and transmission scans by tracking the position of a specially designed goggle attached to the thermoplastic mask.

A 30-minute whole-brain emission scan was acquired 10 minutes after the exposure (i.e., 40 minutes after FDG injection) in a 3D acquisition mode for 25.2 cm axial field of view. A 10-minute transmission scan was conducted after the emission scan to acquire data for attenuation correction. Each of the two sessions took about 90 minutes and the total effective dose for two emission scans was about 7.6 mSv for each subject. Blood samples were taken before the exposure, and before and after the PET scans (i.e., 40 and 80 minutes after FDG injection, respectively) to monitor blood glucose level.

Reconstruction: Image estimates with 1.22 mm isotropic voxels were generated using a speed-optimized version of the OP-OSEM-3D algorithm with 16 subsets and 8 iterations (Hong *et al*, 2007). Counting statistics were tolerable regarding the low statistics bias issue of the OP-OSEM-3D reconstruction (Johansson *et al*, 2007). The 30-minute emission data were reconstructed into three 10-minute frames. All the images were corrected for attenuation, scattering and random events, scanner dead time, and detector normalization, and finally calibrated to kBq/mL with decay correction. Head position tracking data were used to ensure precise spatial matching between transmission and emission data.

Preprocessing: The reconstructed PET images were analyzed with the SPM5 version of Statistical Parametric Mapping (Wellcome Department of Cognitive Neurology, London, UK) (Friston *et al*, 2007) implemented in Matlab 7.4.0 (The Mathworks, Inc., Natik, MA, USA). First, within-subject realignment was performed to eliminate possible differences in the head position between scans. Each image was realigned to the first image of the series and the mean realigned image was created. All images were then realigned to the mean image.

Individual MRI images were coregistered to the mean PET images and segmented to extract images of the gray matter. The individual gray matter images were spatially normalized to the gray matter MNI (Montreal Neurological Institute) MRI brain template available in the SPM5. Transformation parameters calculated at this step were then used to spatially normalize the PET images, which were also resliced at the normalization step to a $2 \times 2 \times 2\,mm^3$ voxel size. The normalized PET images were smoothed with the isotropic 16 mm full width at half maximum Gaussian filter.

Statistical analysis

A two-step statistical analysis was performed. First, the PET data were fitted to a general linear model built according to the subject × condition interaction design including 13 subjects and 3 repetitions of 2 conditions. Differences in global signals were eliminated with proportional scaling of brain voxel values to their mean. Contrast images of intercondition difference were calculated for each individual and entered into the second level analysis treating subjects as a random factor to make inferences at the population level (Penny and Holmes, 2004). Considering a moderate group size, the random-effect analysis was conducted with the permutation-based SnPM5 (Statistical Nonparametric Mapping) (Nichols and Holmes, 2002). The analysis included 1,024 permutations and 10 mm variance smoothing (one-sample pseudo *t*-test), resulting in maps of pseudo *t*-statistic (t_p) values.

Having no prediction about spatial properties of local metabolic effects, we estimated them using a meta-combined, or combo, *w*-statistics that equally weights cluster extent and peak height (Hayasaka and Nichols, 2004) with the $P < 0.05$ significance threshold corrected for multiple comparisons. Possible relationship between intercondition differences in task performance and relative

CMRglu was checked by entering a vector of individual differences in mean reaction times into a separate SnPM simple regression analysis with the same processing parameters as above. Similar analyses were performed for temperature differences in three measurement locations (left eye corner, right eye corner, and right cheek) that showed significant temperature rise.

These analyses were repeated for the volume-of-interest (VOI) including the right temporal cortex that had highest SAR values due to proximity to the active phone (Figure 3). The right temporal VOI containing 19,232 voxels (154 cm^3) included the superior, middle, inferior, Heschl's, and parahippocampal gyri, hippocampus, amygdala, and a part of the fusiform gyrus limited at about $y = -70$ mm in the spatially normalized brain. The VOI was created with MARINA software (Bender Institute of Neuroimaging, Justus Liebig University Giessen, Giessen, Germany) based on the brain structure atlas by Tzourio-Mazoyer *et al* (2002).

Anatomical localization of the voxels with maximal effects was performed with a standard stereotaxic brain atlas (Talairach and Tournoux, 1988) after appropriate coordinate conversion (http://imaging.mrc-cbu.cam.ac.uk/imaging/MniTalairach).

Results

Distributions of Radiation Energy Absorbed by Brain Tissues

The SAR distribution in the head was evaluated by means of numerical calculations (Figure 3). The maximum SAR_{10g} was 0.74 W/kg in the head and the SAR_{10g} in brain tissue was 0.23 W/kg. The highest proportion of radiation energy was absorbed in the right temporal lobe. The tissue-specific SAR values are given in Table 1. The expanded uncertainty for the evaluated SAR values was ±20%.

Temperature Measurements

Two-way analysis of variance with condition (ON, OFF) and time (1-minute intervals during 30 minutes exposure) as independent variables revealed a main effect of time for each measurement location ($F_{29,348} = 6.585$ to 31.413, $P < 0.0005$, $n = 13$), except for the forehead, indicating a temperature rise as a function of time during both real and sham exposures. This overall temperature rise was apparently induced by poor heat dissipation under the phone bodies. The main effect of condition was also significant for the left eye corner ($F_{29,348} = 1.825$, $P = 0.007$; ON: mean ± s.e.m. = 0.13°C ± 0.04°C, OFF: 0.09 ± 0.06), and right eye corner ($F_{29,348} = 2.086$, $P = 0.001$; ON: 0.26 ± 0.09, OFF: 0.10 ± 0.06) and cheek ($F_{29,348} = 3.683$, $P < 0.0005$; ON: 0.47 ± 0.11, OFF: 0.26 ± 0.04). This indicates a significant temperature rise during real exposure, more pronounced on the exposed right side than on the left.

Three-way analysis of variance with side (LEFT, RIGHT) as an additional independent variable revealed a condition × side interaction ($F_{1,12} = 9.013$, $P = 0.011$) for the cheeks due to the significant temperature rise on the right cheek during real exposure. For the eye corners, significant condition × time ($F_{29,348} = 2.481$, $P < 0.0005$) and side × time

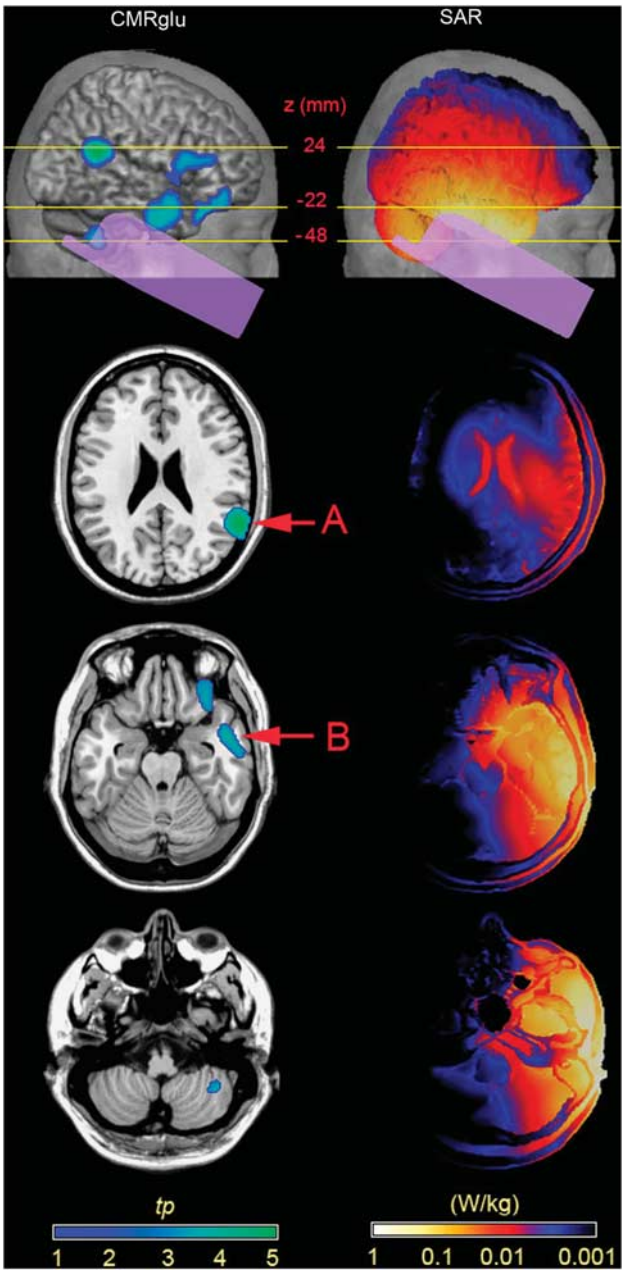

Figure 3 Relative cerebral metabolic rate of glucose (CMRglu) decrease (left column) and specific absorption rate (SAR) distribution (right column) in the presence of Global System for Mobile Communications (GSM) phone exposure. The top row shows the lateral view of the projections of relative CMRglu decreases and superficial SAR distribution in relation to the phone position on the right hemisphere. Horizontal lines indicate the *z* SPM (Statistical Parametric Mapping) coordinates for the three brain slices below. Arrows A and B depict peaks of significant relative CMRglu decreases ($P_{corr} < 0.05$, $n = 13$).

($F_{29,348} = 1.897$, $P = 0.004$) interactions indicated a more pronounced overall temperature rise during real exposure (mean increment ± s.e.m. = 0.36°C ± 0.10°C) than sham exposure (0.16 ± 0.09), and a higher temperature rise on the exposed right side (0.30 ± 0.09) than on the left side (0.22 ± 0.06).

Brain Glucose Consumption

The whole-brain analysis revealed significantly decreased relative CMRglu ($w = 4.10$, $P_{corr} = 0.048$, $n = 13$) during real exposure in the right temporoparietal junction peaking at the border of BAs (Brodmann areas) 40 and 22 at MNI coordinates (x, y, z) 60, −50, 24, corresponding to the SAR_{10g} value of 0.02 W/kg (Figure 3A). The VOI analysis constrained to the right temporal cortex revealed an additional decrease in relative CMRglu during real exposure ($w = 4.10$, $P_{corr} = 0.045$, $n = 13$) in the anterior inferior temporal cortex (BA 20/21) with maximum at MNI coordinates 58, −8, −22 and the SAR_{10g} value of 0.19 W/kg (Figure 3B). Neither the whole-brain nor VOI analyses yielded any areas of relative metabolic increase in the real versus sham comparison. The whole-brain and VOI analysis results are summarized in Table 2.

No significant positive or negative relationship between the intercondition difference in reaction time and relative CMRglu was found in the whole brain or in the VOI. Similarly, no correlation was found between head skin temperature and relative CMRglu differences. Finally, the exposure had no influence on task performance (reaction time, error rate; two-tailed paired t-test, $n = 13$).

Table 1 Tissue-specific SAR values

	SAR_{1g} (mW/kg)	SAR_{10g} (mW/kg)	SAR_{avg} (mW/kg)
Gray matter	380	250	19
White matter	170	98	8.3
Cerebellum	98	62	12
Midbrain	18	11	8.9
Thalamus	10	[a]	8.7
Brain avg.[b]	350	220	14
Total head	2,000	750	22

SAR, specific absorption rate.
[a]Mass of thalamus is < 10 g.
[b]Brain avg. includes gray matter, white matter, cerebellum, midbrain, and thalamus.

Discussion

We found local suppressive effects of a 30-minute exposure to GSM mobile phone on relative CMRglu in the temporal and temporoparietal cortex of the exposed hemisphere. These findings are in line with a previous PET study that reported decreased CBF in the inferior temporal cortex (Aalto *et al*, 2006). The observed suppressive effect on glucose metabolism does not necessarily entail any adverse influence of GSM exposure on brain function because no behavioral effects were found in the present or in many other previous studies (Kwon and Hämäläinen, 2011). Temperature rise was observed on the exposed side of the head, but the magnitude of temperature increase, measured at the skin level, was too small (< 0.21°C) to affect the brain tissue (Van Leeuwen *et al*, 1999).

The FDG accumulation in brain cells depends on blood-to-cell transport and intensity of the first phosphorylation, both of which can be modulated by neural activity (Barros *et al*, 2005). Therefore, GSM phone radiation can have a direct influence on the two processes or an indirect influence through modulation of neuronal activity. To our knowledge, there have been no investigations on the effects of GSM radiation on glucose transporter proteins, or glutamate-based modulation of glucose transporter activity in neurons and astrocytes (Loaiza *et al*, 2003; Porras *et al*, 2004). Although there are some data showing that GSM field can modulate activity or expression of various enzyme proteins (Moustafa *et al*, 2001; Ammari *et al*, 2008; Vanderstraeten and Verschaeve, 2008), we are not aware of any similar studies on the hexokinase and glucose-6-phosphatase that are responsible for FDG phosphorylation and FDG-6P hydrolysis, the k3 and k4 constants in the [^{18}F]-FDG kinetic model (Phelps *et al*, 1979), respectively. In theory, an increase of FDG-6P dephosphorylation could lead to a decrease in FDG accumulation rate due to outward (k4)

Table 2 Brain regions demonstrating decrease in FDG uptake rate in the presence of mobile phone radiation

Analysis level	*Brain area*	*Combo*	*Voxel*	*Peak voxel*	*Peak MNI coordinates (mm)*		
		P_{corr}	P_{corr}	t_p	x	y	z
Whole brain	Supramarginal gyrus (BA 40)	0.048	0.038	5.13	60	−50	24
Right temporal VOI	Inferior temporal gyrus (BA 20)	0.045	0.95	3.83	58	−8	−28
	Middle temporal gyrus (BA 21)		0.97	3.80	50	2	−22

BA, Brodmann area; FDG, ^{18}F-deoxyglucose; MNI, Montreal Neurological Institute; VOI, volume-of-interest.
The MNI coordinates, pseudo t value (t_p), and related FWE-corrected P values (voxel P_{corr}) are reported along with the corrected P value for the combined cluster-voxel w-statistic (combo P_{corr}).

transport that would explain the effect observed in the present study.

Considering possible neural mediation of the observed suppressive effects, ion-based cellular processes could be involved. For example, changes in intracellular Ca^{2+} serve as critical messengers in many cellular processes including neural depolarization. However, attempts to find an influence of a 30-minute 900 MHz GSM exposure on homeostasis of intracellular Ca^{2+} have produced null results even with higher than typical field strengths (O'Connor *et al*, 2010). Considering the complex cellular mechanisms of brain glucose consumption and lack of relevant *in vitro* studies, it is currently not possible to suggest any exposure-sensitive factors in the FDG accumulation mechanism to explain the suppressive effects observed in the present PET study.

A recent PET study (Volkow *et al*, 2011) used a similar FDG method and found increased CMRglu after a 50-minute mobile phone exposure. This study evoked much criticism and discussion (Kosowsky *et al*, 2011; Davis and Balzano, 2011; Nordström, 2011; see also Volkow and coauthors' reply in the same issue). The contradictory results between Volkow *et al* and the present study call for replication. Nevertheless, the present study has several methodological advantages, especially accurate SAR assessment, well-controlled exposure setup, measurement of temperature in the head region, and objective monitoring of the subject's alertness state. Proper dosimetry (Kuster *et al*, 2004) is crucial in microwave exposure studies. Furthermore, confounding factors such as subliminal noise (Haarala *et al*, 2003), pulsed magnetic field from the battery (Jokela *et al*, 2004), or heating of the phone body due to battery or electronic circuit operation must be taken into account. A modified phone was used in this study to avoid temperature rise of the phone chassis and any electrical or acoustic artifacts that could stimulate the brain or give subjects a clue to the exposure status.

In conclusion, our study revealed local suppressive effect of short-term GSM radiation on brain glucose consumption in anterior and posterior parts of the right temporal cortex ipsilateral to the radiation source. While the underlying mechanisms of these effects on local glucose metabolism in the brain remain to be clarified, the present setup rules out changes in skin temperature, acoustic stimulus emanating from the active phone, and changes in the subjects' alertness as potential confounding factors.

Acknowledgements

The authors are very grateful to physicians (Jukka Kemppainen, Gaber Komar, Riitta Parkkola, Timo Suotunen, and Jere Virta) and radiographers (Minna Aatsinki, Heidi Betlehem, Anne-Mari Jokinen, Tarja Keskitalo, Leena Lehtimäki, Hannele Lehtinen, and Kaleva Mölsä) at Turku PET centre. The authors are also grateful to Tim Toivo and Tuomas Mustonen at STUK for carrying out the SAR and return loss measurements.

Disclosure/conflict of interest

The authors declare no conflict of interest.

References

Aalto S, Haarala C, Brück A, Sipilä H, Hämäläinen H, Rinne JO (2006) Mobile phone affects cerebral blood flow in humans. *J Cereb Blood Flow Metab* 26:885–90

Ammari M, Lecomte A, Sakly M, Abdelmelek H, de-Seze R (2008) Exposure to GSM 900 MHz electromagnetic fields affects cerebral cytochrome c oxidase activity. *Toxicology* 250:70–4

Barros LF, Porras OH, Bittner CX (2005) Why glucose transport in the brain matters for PET. *Trends Neurosci* 28:117–9

Boutry CM, Kuehn S, Achermann P, Romann A, Keshvari J, Kuster N (2008) Dosimetric evaluation and comparison of different RF exposure apparatuses used in human volunteer studies. *Bioelectromagnetics* 29:11–9

Chang JY, Duara R, Barker W, Apicella A, Finn R (1987) Two behavioral states studied in a single PET/FDG procedure: theory, method, and preliminary results. *J Nucl Med* 28:852–60

Christ A, Kainz W, Hahn EG, Honegger K, Zefferer M, Neufeld E, Rascher W, Janka R, Bautz W, Chen J, Kiefer B, Schmitt P, Hollenbach HP, Shen JX, Oberle M, Szczerba D, Kam A, Guag JW, Kuster N (2010) The Virtual Family—development of surface-based anatomical models of two adults and two children for dosimetric simulations. *Phys Med Biol* 55:N23–38

Croft RJ, Chandler JS, Burgess AP, Barry RJ, Williams JD, Clarke AR (2002) Acute mobile phone operation affects neural function in humans. *Clin Neurophysiol* 113:1623–32

Croft RJ, Hamblin DL, Spong J, Wood AW, McKenzie RJ, Stough C (2008) The effect of mobile phone electromagnetic fields on the alpha rhythm of human electroencephalogram. *Bioelectromagnetics* 29:1–10

Curcio G, Ferrara M, Moroni F, D'Inzeo G, Bertini M, De Gennaro L (2005) Is the brain influenced by a phone call? An EEG study of resting wakefulness. *Neurosci Res* 53:265–70

Davis CC, Balzano Q (2011) Cell phone activation and brain glucose metabolism. *JAMA* 305:2066–7

Edelstyn N, Oldershaw A (2002) The acute effects of exposure to the electromagnetic field emitted by mobile phones on human attention. *Neuroreport* 13:119–21

Fox PT, Raichle ME, Mintun MA, Dence C (1988) Nonoxidative glucose consumption during focal physiologic neural activity. *Science* 241:462–4

Friston KJ, Ashburner JT, Kiebel SJ, Nochols TE, Penny WD (2007) *Statistical Parametric Mapping: The Analysis of Functional Brain Images*. London, UK: Academic Press

Gabriel C (1996) *Compilation of the Dielectric Properties of Body Tissues at RF and Microwave Frequencies. Technical Report AL/OE-TR-1996-0037*. San Antonio, TX: Brooks Air Force Base

Haarala C, Aalto S, Hautzel H, Julkunen L, Rinne JO, Laine M, Krause B, Hämäläinen H (2003) Effects of a

902 MHz mobile phone on cerebral blood flow in humans: a PET study. *Neuroreport* 14:2019–23

Harris ML, Julyan P, Kulkarni B, Gow D, Hobson A, Hastings D, Zweit J, Hamdy S (2005) Mapping metabolic brain activation during human volitional swallowing: a positron emission tomography study using [^{18}F]fluorodeoxyglucose. *J Cereb Blood Flow Metab* 25:520–6

Hayasaka S, Nichols TE (2004) Combining voxel intensity and cluster extent with permutation test framework. *NeuroImage* 23:54–63

Hietanen M, Kovala T, Hämäläinen A-M (2000) Human brain activity during exposure to radiofrequency fields emitted by cellular phones. *Scand J Work Environ Health* 26:87–92

Hong IK, Chung ST, Kim HK, Kim YB, Son YD, Cho ZH (2007) Ultra fast symmetry and SIMD-based projection-backprojection (SSP) algorithm for 3-D PET image reconstruction. *IEEE Trans Med Imaging* 26: 789–803

Huber R, Treyer V, Borbely AA, Schuderer J, Gottselig JM, Landolt HP, Werth E, Berthold T, Kuster N, Buck A, Achermann P (2002) Electromagnetic fields, such as those from mobile phones, alter regional cerebral blood flow and sleep and waking EEG. *J Sleep Res* 11:289–95

Huber R, Treyer V, Schuderer J, Berthold T, Buck A, Kuster N, Landolt HP, Achermann P (2005) Exposure to pulse-modulated radio frequency electromagnetic fields affects regional cerebral blood flow. *Eur J Neurosci* 21:1000–6

International Electrotechnical Commission (IEC) (2005) *Human Exposure to Radio Frequency Fields from Hand-Held and Bodymounted Wireless Communication Devices—Human Models, Instrumentation, and Procedures—Part 1: Procedure to Determine the Specific Absorption Rate (SAR) for Hand-Held Device Used in Close Proximity to the Ear (Frequency Range of 300 MHz to 3 GHz)*. Geneva, Switzerland: International standard IEC 62209-1 (2005-02)

Johansson J, Oikonen V, Teras M (2007) Quantitative brain imaging using the new, fast iterative histogram-mode reconstruction for the HRRT PET scanner. *IEEE Nucl Sci Symp Conf Rec* 5:3463–7

Jokela K, Puranen L, Sihvonen A-P (2004) Assessment of the magnetic field exposure due to the battery current of digital mobile phones. *Health Phys* 86:56–99

Kleinlogel H, Dierks T, Koenig T, Lehmann H, Minder A, Berz R (2008) Effects of weak mobile phone-electromagnetic fields (GSM, UMTS) on well-being and resting EEG. *Bioelectromagnetics* 29:479–87

Koivisto M, Krause CM, Revonsuo A, Laine M, Hämäläinen H (2000*a*) The effects of electromagnetic field emitted by GSM phones on working memory. *Neuroreport* 11:1641–3

Koivisto M, Revonsuo A, Krause C, Haarala C, Sillanmäki L, Laine M, Hämäläinen H (2000*b*) Effects of 902 MHz electromagnetic field emitted by cellular telephones on response times in humans. *Neuroreport* 11:413–5

Kosowsky A, Swanson E, Gerjuoy E (2011) Cell phone activation and brain glucose metabolism. *JAMA* 305: 2066

Kuster N, Schuderer J, Christ A, Futter P, Ebert S (2004) Guidance for exposure design of human studies addressing health risk evaluations of mobile phones. *Bioelectromagnetics* 25:524–9

Kwon MS, Hämäläinen H (2011) Effects of mobile phone electromagnetic fields: critical evaluation of behavioral and neurophysiological studies. *Bioelectromagnetics* 32:253–72

Loaiza A, Porras OH, Barros LF (2003) Glutamate triggers rapid glucose transport stimulation in astrocytes as evidenced by real-time confocal microscopy. *J Neurosci* 23:7337–42

Mizuno Y, Moriguchi Y, Hikage T, Terao Y, Ohnishi T, Nojima T, Ugawa Y (2009) Effects of W-CDMA 1950 MHz EMF emitted by mobile phones on regional cerebral blood flow in humans. *Bioelectromagnetics* 30:536–44

Moustafa YM, Moustafa RM, Belacy A, Abou-El-Ela SH, Ali FM (2001) Effects of acute exposure to the radiofrequency fields of cellular phones on plasma lipid peroxide and antioxidase activities in human erythrocytes. *J Pharm Biomed Anal* 26:605–8

Nichols TE, Holmes AP (2002) Nonparametric permutation tests for functional neuroimaging: a primer with examples. *Hum Brain Mapp* 15:1–25

Nordström CH (2011) Cell phone activation and brain glucose metabolism. *JAMA* 305:2067

O'Connor RP, Madison SD, Leveque P, Roderick HL, Bootman MD (2010) Exposure to GSM RF fields does not affect calcium homeostasis in human endothelial cells, rat pheocromocytoma cells or rat hippocampal neurons. *PLoS One* 5:e11828

Penny WD, Holmes AJ (2004) Random effect analysis. In: *Human Brain Function* (Frackowiak RSJ, Friston KJ, Frith CD, Dolan RJ, Price CJ, Zeki S, Ashburner JT, Penny WD, eds). 2nd ed. Boston, MA: Elsevier Academic Press, 843–50

Perentos N, Croft RJ, McKenzie RJ, Cvetkovic D, Cosic I (2007) Comparison of the effects of continuous and pulsed mobile phone like RF exposure on the human EEG. *Australas Phys Eng Sci Med* 30:274–80

Phelps ME, Huang SC, Hoffman EJ, Selin C, Sokoloff L, Kuhl DE (1979) Tomographic measurement of local cerebral glucose metabolic rate in humans with (F-18)2-fluoro-2-deoxy-D-glucose: validation of method. *Ann Neurol* 6:371–88

Porras OH, Loaiza A, Barros LF (2004) Glutamate mediates acute glucose transport inhibition in hippocampal neurons. *J Neurosci* 24:9669–73

Preece AW, Iwi G, Davies-Smith A, Wesnes K, Butler S, Lim E, Varey A (1999) Effect of a 915-MHz simulated mobile phone signal on cognitive function in man. *Int J Radiat Biol* 75:447–56

Regel SJ, Gottselig JM, Schuderer J, Tinguely G, Rétey JV, Kuster N, Landolt H-P, Achermann P (2007) Pulsed radio frequency radiation affects cognitive performance and the waking electroencephalogram. *Neuroreport* 18:803–7

Röschke J, Mann K (1997) No short-term effects of digital mobile radio telephone on the awake human electroencephalogram. *Bioelectromagnetics* 18:172–6

Talairach J, Tournoux P (1988) *Co-Planar Stereotaxic Atlas of the Human Brain*. New York, NY: Thieme Medical Publishers

Tzourio-Mazoyer N, Landeau B, Papathanassiou D, Crivello F, Etard O, Delcroix N, Mazoyer B, Joliot M (2002) Automated anatomical labeling of activations in SPM using a macroscopic anatomical parcellation of the MNI MRI single-subject brain. *Neuroimage* 15:273–89

Van Leeuwen GMJ, Lagendijk JJW, Van Leersum BJAM, Zwamborn APM, Hornsleth SN, Kotte ANTJ (1999) Calculation of change in brain temperatures due to exposure to a mobile phone. *Phys Med Biol* 44:2367–79

Vanderstraeten J, Verschaeve L (2008) Gene and protein expression following exposure to radiofrequency fields from mobile phones. *Environ Health Perspect* 116:1131–5

Volkow ND, Tomasi D, Wang G-J, Vaska P, Fowler JS, Telang F, Alexoff D, Logan J, Wong C (2011) Effects of cell phone radiofrequency signal exposure on brain glucose metabolism. *JAMA* 305:808–13

Wienhard K, Schmand M, Casey M, Baker K, Bao J, Eriksson L, Jones W, Knoess C, Lenox M, Lercher M, Luk P, Michel C, Reed J, Richerzhagen N, Treffert J, Vollmar S, Young J, Heiss W, Nutt R (2002) The ECAT HRRT: performance and first clinical application of the new high resolution research tomograph. *IEEE Trans Nucl Sci* 49:104–10